Geochemical Perspectives Letters

Triple oxygen isotopes of meteoric hydrothermal systems – implications for palaeoaltimetry

C.P. Chamberlain[1*,+], D.E. Ibarra[1,2+], M.K. Lloyd[2], T. Kukla[1], D. Sjostrom[3], Y. Gao[1,4], Z.D. Sharp[5]

doi: 10.7185/geochemlet.2026

Abstract

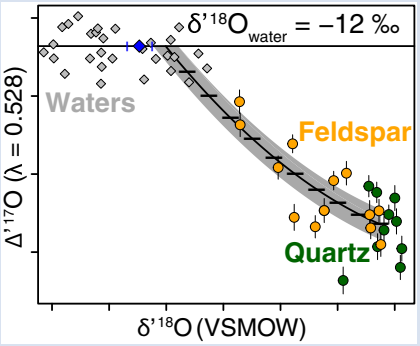

We use triple oxygen isotopes of altered granitic rocks to determine the isotope composition of meteoric waters in a fossil hydrothermal system, the low $\delta^{18}O$ Eocene Idaho Batholith, originally studied by Criss and Taylor (1983). In doing so we: 1) test whether meteoric water values estimated from previous $\delta^{18}O$ and δD analyses on quartz, feldspar and biotite are robust and 2) determine the palaeoelevation of the Eocene highlands that are presently constrained primarily by the $\delta^{18}O$ and δD of paired muscovite and quartz from core complexes and altered granites.

Our calculated $\delta^{18}O$ values of meteoric water are higher than estimates that use combined feldspar $\delta^{18}O$ and biotite δD measurements in these hydrothermally altered granites and δD values from muscovite from nearby core complexes (Mulch *et al.*, 2004). Both methods are consistent with a high elevation (~3.1 to 4.7 km) Eocene highland in the northwestern U.S. Cordillera.

Received 7 March 2020 | Accepted 26 May 2020 | Published 28 July 2020

Introduction

With the advent of stable isotope palaeoaltimetry it has been possible to determine the past elevations of the worlds major mountain belts by exploiting the relationship between $\delta^{18}O$ and δD of meteoric waters and elevation as described by Rayleigh distillation over orography (Poage and Chamberlain, 2001; Rowley *et al.*, 2001). Multiple proxies for the isotopic composition of meteoric waters have been used for these elevation reconstructions. These include the δD of 1) organic molecules from fossilised leafs (Hren *et al.*, 2010), hydrated volcanic glasses (Mulch *et al.*, 2008), pedogenic clays (Chamberlain *et al.*, 1999), hydrothermal micas (Mulch *et al.*, 2004), fluid inclusions of quartz veins (Sharp *et al.*, 2005); and the $\delta^{18}O$ of 2) pedogenic and lacustrine carbonate (Quade *et al.*, 2007), lacustrine chert (Davis *et al.*, 2009), and pedogenic clays (Mix and Chamberlain, 2014). While these proxies are excellent predictors of the isotopic composition of meteoric waters they are limited by their geographic location as many occur only in the sedimentary basins that flank the crystalline cores of mountain belts. Nowhere is this more prevalent than in the North American Cordillera where almost all palaeoelevation estimates come from intermontane basins that are adjacent to crystalline uplifts (Chamberlain *et al.*, 2012; Fig. 1).

Most determinations of the isotopic composition of meteoric waters using crystalline rocks rely on the δD of micas from hydrothermally altered rocks within fault zones (Mulch *et al.*, 2004) or altered granites (Criss and Taylor, 1983). A potential problem with this approach is that hydrogen isotopes of phyllosilicates may continue to exchange well after crystallisation. For example, O'Neil and Kharaka (1976) showed that exchange of hydrogen, but not oxygen, occurred in clay minerals at temperatures above 100 °C. It is also possible that micas may be exchanging H rather than OH groups and that this exchange occurs at temperatures typical of cooling crystalline rocks. If this is the case, then the oxygen and hydrogen isotope values of micas may be decoupled and cooling rate dependent (Graham *et al.*, 1987). Hence, the motivation of this study is to use triple oxygen isotopes to determine the isotopic composition of meteoric waters. Unlike the H-O system, the $^{17}O/^{16}O$ and $^{18}O/^{16}O$ systems are not decoupled, and should change in concert during alteration.

To estimate the isotopic compositon of meteoric water in a hydrothermal system, we modify the approach of Herwartz *et al.* (2015) who used arrays of triple oxygen isotopes on a suite of rocks to determine the $\delta^{18}O$ of alteration waters during a Snowball Earth event (see also Zakharov *et al.*, 2017). Here, we use mixing equations (Taylor, 1978) modified for ^{17}O to

1. Geological Sciences, Stanford University, Stanford, California 94305, USA
2. Earth and Planetary Science, UC Berkeley, Berkeley, California 94720s, USA
3. Geology Program, Rocky Mountain College, Billings, Montana 59102, USA
4. Earth Sciences and Resources, China University of Geosciences (Beijing), Beijing, 100083 China
5. Earth and Planetary Sciences, University of New Mexico, Albuquerque, New Mexico 87131, USA
* Corresponding author (email: chamb@stanford.edu)
\+ C.P. Chamberlain and D.E. Ibarra contributed equally to this work.

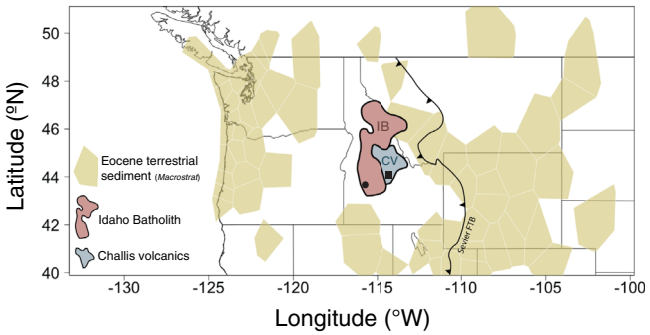

Figure 1 Map of Idaho batholith and surrounding Eocene basins. Symbols represent the study area (dot), and the Pioneer core complex (square).

determine the palaeoelevation of Eocene hydrothermally altered rocks of the Idaho batholith (Criss and Taylor, 1983). We show that triple oxygen isotopes correspond to Eocene meteoric water values that are higher than those determined by hydrogen isotope analysis, suggesting that retrograde hydrogen, but not oxygen, isotope exchange has occurred between micas and fluids.

Geologic Setting

The Idaho batholith (~25 000 km^2) lies within the crystalline core of the North American Cordillera. It is flanked on both the west and east by Cenozoic intermontane basins that contain debri eroded from the batholith and surrounding rocks (Fig. 1). The batholith is Cretaceous to Eocene in age and consists of granites and granodiorites (Gaschnig *et al.*, 2010). The batholith was hydrothermally altered during the emplacment of the Eocene plutons and eruption of the Challis volcanics. Using hydrogen and oxygen isotopes of minerals from these Eocene granites, Criss and Taylor (1983) demonstrated that the hydrothermal systems consisted of meteoric waters within flow systems centred on the Eocene plutons. The hydrothermal centre targeted here, the Rocky Bar complex, lies in the southwest corner of the Idaho Batholith.

The Rocky Bar complex was emplaced (~48 Ma; Gaschnig *et al.*, 2010) and hydrothermally altered (~45 to 37 Ma; Criss *et al.*, 1982) during the Eocene. The alteration of the pluton and wallrocks is evidenced by low $\delta^{18}O$ values of plagioclase (down to −2.5 ‰), with the lowest values occuring near the core of the pluton and along the faults that ring the complex. Guided by the results of Criss and Taylor (1983), we collected granites from the Rocky Bar complex exposed along Highway 21 that transects the complex (Table S-1).

Results

Our analysis of $\delta^{18}O$, $\delta^{17}O$ of plagioclase and quartz, and δD of biotite give three results, which are:

First, the $\delta^{18}O$ of plagioclase has larger variations than that of quartz. The $\delta^{18}O$ of plagioclase ranges from −3.6 to 8.8 ‰; quartz $\delta^{18}O$ values range from 5.5 to 10.7 ‰ (Table S-1). Moreover, the $\delta^{18}O$ of coexisiting mineral pairs form disequilibrium arrays (Fig. 2) similar to those discovered by Criss and Taylor (1983). Second, the $\Delta'^{17}O$ ($\delta'^{17}O - 0.528 \times \delta'^{18}O$) of plagioclase, like the $\delta^{18}O$ values, show a wider range than that of quartz. $\Delta'^{17}O$ of plagioclase ranges from −0.004 to −0.095, and $\Delta'^{17}O$ of quartz ranges from −0.058 to −0.118. Third, the $\delta^{18}O$ of feldspar and δD values of biotite also form a water-rock mixing array (Fig. 4, Table S-1).

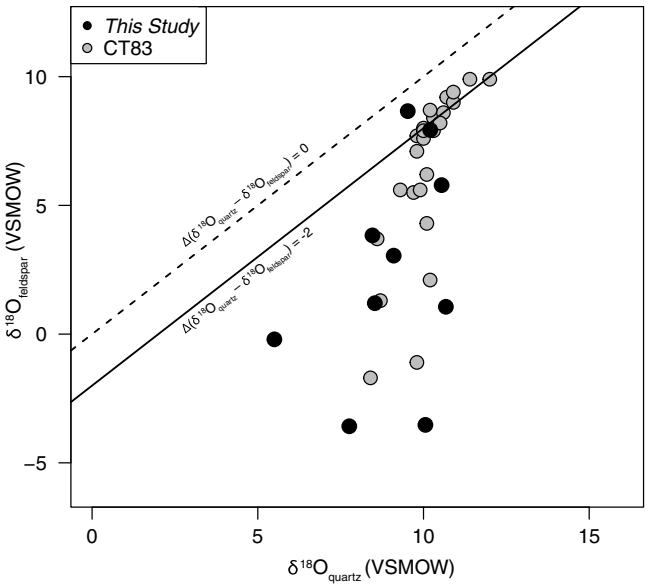

Figure 2 $\delta^{18}O_{quartz}$ *versus* $\delta^{18}O_{plagioclase}$ for coexisiting mineral pairs. Black dots are this study and gray dots those of Criss and Taylor (1983). Shown are the $\Delta_{qtz\text{-}plag}$ for 0 and 2.0 ‰. 2.0 ‰ is the equilibrium fractionation between quartz and feldpsar for granitic rocks (O'Neil and Taylor, 1967).

Interpretation

Our results agree with the interpretation that the oxygen and hydrogen isotopes reflect a high temperature hydrothermal system during emplacment of the Eocene plutons (Criss and Taylor, 1983). Disequilibrium arrays of the oxygen isotopes of paired quartz and plagioclase (Fig. 2) result from differential exchange between fluids and quartz/feldspar during hydrothermal activity, with feldspar exchanging more rapidly than quartz. These kinetic controls are also reflected in the $\Delta'^{17}O$ values.

The kinetic effects are evidenced by the wide range of $\lambda_{quartz\text{-}feldspar}$ values. Note that, following Pack and Herwartz (2014) and Sharp *et al.* (2018), we use θ to represent the theoretical slope, whereas λ is used to represent the empirical slope using data. As stated above our $\lambda_{quartz\text{-}feldspar}$ values range from 0.5152 to 0.5305 (Table S-1). The theoretical high temperature slope is $\theta = 0.5305$ (Young *et al.*, 2002). Given the wide range of $\lambda_{quartz\text{-}feldspar}$ values (Table S-1) and the narrow temperature range experienced by these granites and high temperature fluids it is highly unlikely that these minerals are in isotopic equilibrium. Thus, our results are consistent with the interpretation of Criss and Taylor (1983), but with the added constraint that we can calculate the meteoric water composition using oxygen isotopes alone.

To determine the oxygen isotopic composition of meteoric water we used the array of $\delta'^{18}O$ and $\Delta'^{17}O$ (Fig. 3) values for plagioclase. A fit through this array (see Supplementary Information) using the water-rock equations of Taylor (1978) assuming a 400 °C alteration temperature, gives a value of $\delta^{18}O$ of meteoric water of −11.99 ‰ (±1.11, 1σ). Propagating the uncertainty around the meteoric water line of Passey and Ji (2019) (dashed lines in Fig. 3) and the best fit regression shown in Figure 3, produces a field spanning −10 to −15 ‰ (see Table S-2). Additionally, if the feldspar-H_2O interaction is set to a colder temperature, such as 250 °C, rather than the maximum 400 °C assumed by Criss and Taylor (1983), we calculate a $\delta^{18}O$ of meteoric water of −15 ‰ (Fig. S-1). However, this lower temperature is probably unreasonable given that it is below the closure temperature of the dated hydrothermal micas

(Criss and Taylor, 1983). Regardless, it is clear that the Eocene meteoric water has a low $\delta^{18}O$ value. However, our $\delta^{18}O$ value is higher than that determined previously (approximately −16 ‰) by Criss and Taylor (1983) who use both $\delta^{18}O$ and δD values. Our $\delta^{18}O$-δD data give results similar to Criss and Taylor (1983) with a best fit to the data of $\delta^{18}O = -15.25$ ‰ (±1.12, 1σ; Fig. 4).

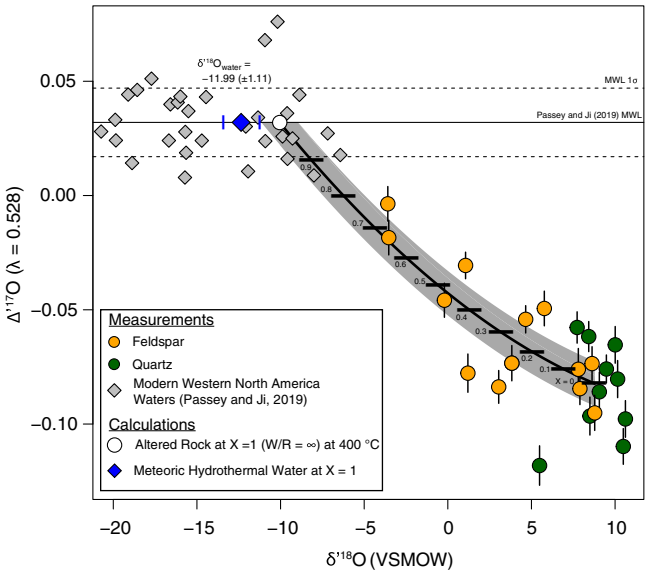

Figure 3 The $\delta'^{18}O$–$\Delta'^{17}O$ alteration relationship of feldspar used to derive meteoric water. Meteoric water lines and compiled modern water data are from Passey and Ji (2019). Given are the 1 s.e. bars for the measurements. The black line is the alteration array between unaltered rock and rock in equilibrium with the metoric water fit to the feldspar data for fractional mixing (Taylor, 1978).

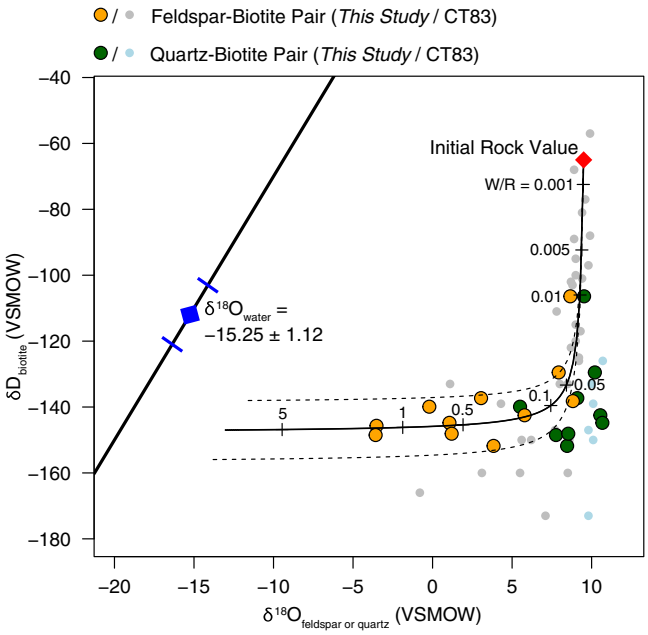

Figure 4 The $\delta^{18}O$–δD array for feldspar-biotite (this study; Criss and Taylor, 1983) with water/rock (W/R) values of the molar fraction of oxygen given the best fit meteoric water value. W/R values assume fractionation factors of feldspar-H_2O = +2 ‰ for $\delta^{18}O$ and biotite-H_2O = −35 ‰ for δD (Taylor, 1977). Quartz values were not used for calculations.

Discussion and Conclusions

Most estimates of the isotopic composition of meteoric waters that interacted with crystalline rocks rely on the hydrogen isotope composition of the altered rocks. The isotopic composition of these waters is either calculated directly from δD values of hydrous minerals and using temperatures from oxygen isotope thermometry (Mulch *et al.*, 2004) or from combined oxygen and hydrogen isotope analyses of rocks and their hydrothermally altered end members and the mixing relationships between them (Criss and Taylor, 1983). Because of the possibility of exchange of hydrogen between minerals and later fluids it is a concern that estimates of the original composition of the meteoric water in these hydrothermal systems is compromised. This difference in calculated meteoric water compositons is measurable and can lead to error in estimates of the isotopic composition of meteoric waters during hydrothermal activity. The error then translates directly to error in palaeoelevation estimates, particularly at low elevations.

For example, we demonstrate that based on the extrapolated mixing relationships in triple oxygen isotope space using feldspar analyses give calculated meteoric water values, assuming 400 °C, that are ~2.7 to 3.9 ‰ (Table S-2) higher than those determined using combined oxygen and hydrogen isotopes. We note that this difference in calculated meteoric water values is dependent upon the assumed temperature of the hydrothermal system and the choice of the meteoric water lines in $\delta'^{18}O$ and $\Delta'^{17}O$ space (Table S-1). If we take the maximum temperature of the hydrothermal system of 400 °C (Criss and Taylor, 1983) will this isotopic difference translate into an elevation difference that is significant? To test this we use the data presented here, with that published on nearby Eocene (38 to 37 Ma) Pioneer core complexes (McFadden *et al.*, 2015) and the Idaho batholith (Criss and Taylor, 1983) (Fig. 1). These three studies all differ in their calculation of the isotopic composition of meteoric waters. Ours is based on triple oxygen and the others rely on hydrogen isotopes. McFadden *et al.* (2015) use the δD values of micas from detachment faults active in the late Eocene and assumed temperature of formation of these detachments and calculate a $\delta^{18}O$ of meteoric water of −16.0 ± 1.5 ‰. Criss and Taylor (1983) use δD of biotites and muscovite and the $\delta^{18}O$ of feldspar and vein quartz and arrive at the same $\delta^{18}O$ of meteoric water of −16 ‰. Using the equations for Eocene lapse rates of Rowley *et al.* (2001), the Eocene elevation of the Idaho batholith was 4.74 km (+0.64/−0.49, 1σ of the Rowley model) based on hydrogen isotopes. Using the best fit of meteoric water at 400 °C alteration temperature (−11.92 ‰) we estimate a lower Eocene elevation of 3.11 km +0.31/−0.38 (1σ), based on triple oxygen isotopes. At 1σ and even at 2σ these values do not overlap, though they do overlap at 2σ using other meteoric water lines (Table S-2). Nonetheless, we suggest that later hydrogen exchange, at least in this case, results in inaccurate palaeoelevation estimates.

Acknowledgements

This research was funded by NSF EAR-1322084 and Heising Simons grants to CPC. DEI was supported by Miller Research Institute and UC President's Postdoctoral Fellowships. MKL was supported by the Agouron Institute Geobiology Fellowship. We thank Daniel Herwartz and Andreas Pack for reviews.

Editor: Eric H. Oelkers

Additional Information

Supplementary Information accompanies this letter at http://www.geochemicalperspectivesletters.org/article2026.

Cite this letter as: Chamberlain, C.P., Ibarra, D.E., Lloyd, M.K., Kukla, T., Sjostrom, D., Gao, Y., Sharp, Z.D. (2020) Triple oxygen isotopes of meteoric hydrothermal systems – implications for palaeoaltimetry. *Geochem. Persp. Let.* 15, 6–9.

References

Chamberlain, C.P., Poage, M., Craw, D., Reynolds, R. (1999) Topographic development of the Southern Alps recorded by the isotopic composition of authigenic clay minerals, South Island, New Zealand. *Chemical Geology* 155, 279–294.

Chamberlain, C.P., Mix, H.T., Mulch, A., Hren, M.T., Kent-Corson, M.L., Davis, S.J., Horton, T.W., Graham, S.A. (2012) The Cenozoic climatic and topographic evolution of the western North American Cordillera. *American Journal of Science* 312, 213–262.

Criss, R.R., Taylor, H.P. Jr. (1983) An $^{18}O/^{16}O$ and D/H study of Tertiary hydrothermal system in the southern half of the Idaho batholith. *Geological Society of America Bulletin* 94, 640–663.

Criss, R.E., Lanphere, M.A., Taylor, H.P. Jr. (1982) Effects of regional uplift, deformation and meteoric-hydrothermal metamorphism on K-Ar ages of biotites in the southern half of the Idaho Batholith. *Journal of Geophysical Research* 87, 7026–7046.

Davis, S.J., Mulch, A., Caroll, A.R., Horton, T.W., Chamberlain, C.P. (2009) Paleogene landscape evolution of the central North American Cordillera: Developing topography and hydrology in the Laramide foreland. *Geological Society of America Bulletin* 121, 100–116.

Gaschnig, R.M., Vervoort, J.D., Lewis, R.S., McClelland, W.C. (2010) Migrating magmatism in the northern US Cordillera: in situ U-Pb geochronology of the Idaho batholith. *Contributions to Mineralogy and Petrology* 159, 863–883.

Graham, C.M., Viglino, J.A., Harmon, R.S. (1987) Experimental study of hydrogen-isotope exchange between aluminous chlorite and water and of hydrogen diffusion in chlorite. *American Mineralogist* 72, 566–579.

Herwartz, D., Pack, A., Krylov, D., Xiao, Y., Muehlenbachs, K., Sengupta, S., Di Rocco, T. (2015) Revealing the climate of snowball Earth from $\Delta^{17}O$ systematics of hydrothermal rocks. *Proceedings of the National Academy of Sciences* 112, 5337–5341.

Hren, M.T., Pagani, M., Erwin, D.M., Brandon, M. (2010) Biomarker reconstruction of the early Eocene paleotopography and paleoclimate of the northern Sierra Nevada. *Geology* 38, 7–10.

McFadden, R.R., Mulch, A., Teyssier, C., Heizker, M. (2015) Extension and meteoric fluid flow in the Wildhorse detachment, Pioneer metamorphic core complex, Idaho. *Lithosphere* 7, 355–366.

Mix, H.T., Chamberlain, C.P. (2014) Stable isotopic records of hydrologic change and paleotemperature from smectite in Cenozoic Western North America. *Geochimica et Cosmochimica Acta* 141, 532–546.

Mulch, A., Teyssier, C., Cosca, M.A., Vanderhaeghe, O., Vennemann, T. (2004) Reconstructing paleoelevation in eroded orogens. *Geology* 32, 525–528.

Mulch, A., Sarna-Wojcicki, A.M., Perkins, M.E., Chamberlain, C.P. (2008) A Miocene to Pleistocene climate and elevation record of the Sierra Nevada (California). *Proceedings of the National Academy of Sciences of the United States of America* 105, 6819–6824.

O'Neil, J.R., Taylor, H.P. Jr. (1967) The oxygen isotope and cation exchange chemistry of feldspars. *American Mineralogist* 52, 1414–1437.

O'Neil, J.R., Kharaka, Y.K. (1976) Hydrogen and oxygen isotope exchange reactions between clay minerals and water. *Geochimica et Cosmochimica Acta* 40, 241–246.

Pack, A., Herwartz, D. (2014). The triple oxygen isotope composition of the Earth mantle and understanding ΔO^{17} variations in terrestrial rocks and minerals. *Earth and Planetary Science Letters* 390, 138–145.

Passey, B. H., Ji, H. (2019) Triple oxygen isotope signatures of evaporation in lake waters and carbonates: A case study from the western United States. *Earth and Planetary Science Letters* 518, 1–12.

Poage, M.A., Chamberlain, C.P. (2001) Empirical relationships between elevation and the stable isotope composition of precipitation and surface waters: Considerations for studies of paleoelevation change. *American Journal of Science* 301, 1–15.

Quade, J., Garzione, C., Eiler, J. (2007) Paleoelevation reconstruction using pedogenic carbonates. In: Kohn, M. (Ed.) *Reviews in Mineralogy and Geochemistry* 66, 53–87.

Rowley, D.B., Pierrehumbert, R.T., Currie, B.S. (2001) A new approach to stable isotope-based paleoaltimetry: implications for paleoaltimetry and paleohypsometry of the High Himalaya since the Late Miocene. *Earth and Planetary Science Letters* 188, 253–268.

Sharp, Z.D., Masson, H., Lucchini, R. (2005) Stable isotope geochemistry and formation mechanisms of quartz veins: extreme paleoaltitudes of the central Alps in the Neogene. *American Journal of Science* 305, 187–219.

Sharp, Z.D., Wostbrock, J.A.G., Pack, A. (2018) Mass-dependent triple oxygen isotope variations in terrestrial materials. *Geochemical Perspectives Letters* 7, 27–31.

Taylor, H.P. Jr. (1977) Water/rock interactions and the origin of H_2O in granitic batholiths. *Journal Geological Society of London* 133, 509–558.

Taylor, H.P. Jr. (1978) Oxygen and hydrogen isotope systematics of plutonic granitic rocks. *Earth and Planetary Science Letters* 38, 177–210.

Young, E.D., Galy, A. Nagahara, H. (2002) Kinetic and equilibrium mass-dependent isotope fractionation laws in nature and their geochemical and cosmochemical significance. *Geochimica et Cosmochimica Acta* 66, 1095–1104.

Zakharov, D.O., Bindeman, I.N., Slabunov, A.I., Ovtcharova, M., Coble, M.A., Serebryakov, N.S., Schaltegger, U. (2017) Dating the Paleoproterozoic snowball Earth glaciations using contemporaneous subglacial hydrothermal systems. *Geology* 45, 667–670.

Geochemical Perspectives Letters

Triple oxygen isotopes of meteoric hydrothermal systems – implications for palaeoaltimetry

C.P. Chamberlain, D.E. Ibarra, M.K. Lloyd, T. Kukla, Y. Gao, D.J. Sjostrom, Z.D. Sharp

Supplementary Information

The Supplementary Information includes:

- Supplementary Methods
- Supplementary Equations
- Tables S-1 and S-2
- Figure S-1
- Supplementary Information References

Supplementary Methods

Mineral separates were collected by drilling out phenocrysts and then hand picking under a microscope. All samples were measured at Stanford University using a Thermo 253 Plus 10kV IRMS. The laser fluorination method is that established by Sharp (1990) and Sharp *et al*. (2016). In brief, this method involves pre-fluorinating the sample chamber at 30 Torr multiple times to remove any absorbed water before analysis. After no more non-condensables are liberated we lase the individual minerals. For each sample we use a 130 mbar BrF_5 and heat the sample using a CO_2 infrared laser in a vacuumed fluorination line. Only one feldspar separate was loaded per chamber and feldspar samples were always analyzed first in each session. We found that laser times less than 5 minutes produced the most accurate and precise analyses. Following fluorination, the evolved O_2 gas is passed over a heated NaCl trap to remove any F_2 and SiF_4 produced and then frozen onto a 5Å mol sieve. The sample is then frozen onto a second 5Å mol sieve after passing through a He flow through GC column to remove NF_3 and other contaminants. The purified O_2 aliquot is equilibrated within the 253 Plus bellows for 6 minutes and each bellows cycled several times to assure adequate mixing of the gas. Measurements were made for 1.5 to 3+ hours at 5V on mass $^{32}O_2$ to ensure measurement precision of <0.01 ‰ for $\Delta'^{17}O$. We applied the baseline correction of Yeung *et al*. (2018) and checked this baseline correction about every two weeks. Our reproducibility on sessions where samples from this study are analysed for an internal standard hydrothermal quartz standard L1 is 0.070 ‰ for $\delta'^{18}O$ and 0.016 ‰ for $\Delta'^{17}O$ (n = 23 measurements over 13 months), for UWG-2 (Gore Mountain Garnet) is 0.401 ‰ for $\delta'^{18}O$ and 0.012 ‰ for $\Delta'^{17}O$ (n = 3), and for SCO (San Carlos Olivine, University of New Mexico) is 0.365 ‰ for $\delta'^{18}O$ and 0.005 ‰ for $\Delta'^{17}O$ (n = 5). All of our analyses are relative to published high-precision olivine, garnet and quartz standards; specifically SCO, UWG-2 and L1 values (Pack and Herwartz, 2014; Sharp *et al*., 2016; Wostbrock *et al*., 2018, 2020) that were analysed with each batch of samples (Table S-1).

Supplementary Equations

Stable isotope fractionation between two substances (a and b) is described by the basic equation:

$$\alpha = \frac{R_a}{R_b} \qquad \textbf{Eq. S-1}$$

In this equation R is the ratio of the heavy to light isotope. Here $^{18}O/^{16}O$ and $^{17}O/^{16}O$. The delta notation is:

$$\delta = \left(\frac{R_a}{R_b} - 1\right) \cdot 1000 \qquad \textbf{Eq. S-2}$$

Rearranging equations S-1 and S-2 the alpha value can be expressed as:

$$\alpha_{a-b} = \frac{\delta_a - 1000}{\delta_b - 1000} \qquad \textbf{Eq. S-3}$$

The alpha values for oxygen 17 and 18 are related by their exponent θ, as such:

$$\alpha_{a-b}{}^{17}O = (\alpha_{a-b}{}^{18}O)^{\theta} \qquad \textbf{Eq. S-4}$$

θ varies as a function of equilibrium and kinetic processes (Young *et al.*, 2002) and for equilibrium process it is temperature dependent (Sharp *et al.*, 2016).

Equation S-4 in linear form is:

$$\ln(\alpha^{17}O) = \theta \ln(\alpha^{18}O) \qquad \textbf{Eq. S-5}$$

The linearised values of δ values given by:

$$\delta' = 1000 \cdot \ln\left(\frac{\delta}{1000} + 1\right) \qquad \textbf{Eq. S-6}$$

The θ value for the linearised δ′ value is given as:

$$\theta_{a-b} = \frac{\delta'^{17}O_a - \delta'^{17}O_b}{\delta'^{18}O_a - \delta'^{18}O_b} \qquad \textbf{Eq. S-7}$$

For triple oxygen isotope analysis we use the deviation of isotope values from the terrestrial isotope fractionation line, which has a slope of ~1/2 in $\delta'^{18}O$ *vs.* $\delta'^{17}O$ space. The terrestrial fractionation line is defined as:

$$\delta'^{17}O = \lambda_{RL}\delta'^{18}O + \gamma_{RL} \qquad \textbf{Eq. S-8}$$

You will note here that θ has been replaced by λ to emphasize the difference between process-based values (θ) and empirical values (λ). The subscript RL refers to the reference line used (see following). The Y intercept of this equation is γ, which is taken as zero. One of the difficulties introduced into comparing triple oxygen results is the selection of which λ to use as these vary between different substances and different processes. Following Sharp et al. (2018) we use a value of 0.528 (λ) in equation S-9.

$$\Delta'^{17}O = \delta'^{17}O - \lambda_{RL}\delta'^{18}O + \gamma_{RL} \qquad \textbf{Eq. S-9}$$

For individual hand sample mineral pairs (quartz-feldspar) we calculate apparent $\lambda_{\text{quartz-feldspar}}$ values following equation S7. We denote this using λ as this slope may represent mixing or non-equilibrium (*i.e.* kinetically controlled) processes during fluid-rock interaction, whereby the plagioclase is more exchanged than the quartz.

To calculate the end-member alteration waters (*i.e.* hydrothermal waters derived from meteoric waters at infinite fluid/rock interaction) we modify the approach of Herwartz *et al.* (2015) (see also Zakharov *et al.*, 2017) using equations originally presented by Taylor (1978). Using a simple mass-balance mixing model, the fraction of water (X) allowed to equilibrate with a rock at a given temperature gives the bulk composition by the equations (where $\delta^x O$ is for $\delta^{17}O$ or $\delta^{18}O$):

$$\delta^x O_{bulk} = X_{water}\,(\delta^x O_{water,initial}) + (1\text{-}X_{water})\,(\delta^x O_{rock,initial}) \qquad \textbf{Eq. S-10}$$

$$\delta^x O_{bulk} = X_{water}\,(\delta^x O_{water,final}) + (1\text{-}X_{water})\,(\delta^x O_{rock,final}) \qquad \textbf{Eq. S-11}$$

$\delta^x O$ can be either $\delta^{18}O$ or $\delta^{17}O$. The final $\delta^x O$ value of the rock is determined by the additional equation:

$$\alpha^x = \frac{1000 + \delta^x O_{\text{final rock}}}{1000 + \delta^x O_{\text{final water}}} \qquad \textbf{Eq. S-12}$$

This leads to the relationship between the initial rock and water oxygen isotope compositions, the fluid/rock ratio and the final isotopic composition of the rock:

$$\delta^x O_{rock\ final} = \frac{1000X + \alpha\left(X \cdot \delta^x O_{rock\ initial} - X \cdot \delta^x O_{water\ initial} - \delta^x O_{rock\ initial} - 1000X\right)}{\alpha X - \alpha - X} \qquad \textbf{Eq. S-13}$$

In order to calculate the alteration relationship of the feldspar minerals analysed in this study we use apply the fractionation factor of Matsuhisa *et al*. (1979) assuming the feldspar (plagioclase) analysed here is 20 % Anorthite and 80 % Albite, and the following equations for triple oxygen isotopes to derive the end-members. The equilibrium fractionation for $\delta^{18}O$ between a mineral and water is given by:

$$\delta'^{18} O_{mineral} = \delta'^{18} O_{water} + \frac{a \times 10^6}{T^2} + \frac{b \times 10^3}{T} + c \qquad \textbf{Eq. S-14}$$

where a, b and c are fitted or theoretically derived coefficients (note that b=0 in Matsuhisa *et al*. (1979); a = 2.21 and c = -2.57). Which, given the relationships described above the equilibrium fractionation for $\delta^{17}O$ and $\Delta'^{17}O$, where ε is fitted slope for the temperature dependence of θ; e.g., Sharp *et al*., 2016), is thus:

$$\delta'^{17} O_{mineral} = \delta'^{17} O_{water} + \left(\frac{a \times 10^6}{T^2} + \frac{b \times 10^3}{T} + c\right)\left(0.5305 - \frac{\varepsilon}{T}\right) \qquad \textbf{Eq. S-15}$$

$$\Delta'^{17} O_{mineral} = \delta'^{17} O_{water} - \lambda \cdot \delta'^{18} O_{water} + \left(\frac{a \times 10^6}{T^2} + \frac{b \times 10^3}{T} + c\right)\left(0.5305 - \frac{\varepsilon}{T} - \lambda\right) \qquad \textbf{Eq. S-16}$$

The fitted slope dependence (ε) is set here to 1.7 (quartz-water is 1.85; Sharp *et al*., 2016; Wostbrock *et al*., 2018) based on lower $\delta^{18}O$ fractionation factors (at equivalent temperatures) for feldspar, although no experimental or natural datasets yet exist to assess this value. We note that our calculations are insensitive to ε values ranging from 1.5 to 1.85. Then, combining the equation S-14 and S-16, a relationship between the $\Delta'^{17}O$ and $\delta^{18}O$ for a mineral in equilibrium with water is thus:

$$\Delta'^{17} O = \delta'^{17} O_w + \left(\delta'^{18} O_r - \delta'^{18} O_w\right)\left(0.5305 + \frac{\left(c - \delta'^{18} O_r + \delta'^{18} O_w\right)\varepsilon}{500\left(b + \sqrt{b^2 - 4a\left(c - \delta'^{18} O_r + \delta'^{18} O_w\right)}\right)} - \lambda\right) - \delta'^{18} O_w \cdot \lambda \qquad \textbf{Eq. S-17}$$

Finally, by assuming an end-member initial feldspar values ($\Delta'^{17}O$ = -0.082 and $\delta'^{18}O$ = 8.78) based on our data and temperature (400 °C based on Criss and Taylor, 1983), we derive a best fit to the $\Delta'^{17}O$-$\delta^{18}O$ array of feldspar data (black line on Fig. 3) for equation S-13 (using equation S-17) for fractional mixing (X) of 0 (rock-buffered end-member) to 1 (water-buffered end-member, i.e., fluid/rock of infinity). The best fit (determined via lowest RMSE) and uncertainty on the best fit to this array was assessed using the measurement error (Table S-1) and error on the end-member initial feldspar values via a Monte Carlo routine. Sensitivity to the choice of alteration temperature is shown in Figure S-1 *via* the equation that follows from the above relationships as (excluding b for our purposes, see above):

$$\delta'^{18} O_{water} = \delta'^{18} O_{rock} - c - \frac{a \times 10^6}{T^2} \qquad \textbf{Eq. S-18}$$

Where we approximate the rock $\delta'^{18}O$ to that of the end-member derived from the triple oxygen isotope relationship in Figure 3 ($\delta'^{18}O_{rock,final}$ = -9.68 when X=1). The associated end-member meteoric water uncertainty extrapolated to the meteoric water line of Passey and Ji (2019) is given in Table S-2 and on Figure 3; however, full inclusion of the meteoric water line uncertainty (dashed lines in Figure 3 from Passey and Ji (2019), chosen because those data (grey diamonds on Figure 3) are from western North America) dominate the uncertainty associated with these calculations (range given in main text). Calculations using assumptions of different meteoric water line slopes and intercepts are given in Table S-2 to demonstrate the range of differences given our current knowledge of the meteoric water line.

Supplementary Tables

Table S-1 Triple oxygen isotope and D/H measurements of Idaho Batholite samples. Standards averaged only over sessions when data was produced (December 2018 to December 2019). All oxygen isotope data is normalized to SCO, UWG-2 and L1 values in Wostbrock *et al.* (2020). Biotite δD were measured in triplicate. All values versus VSMOW.

Feldspar Measurements							
Sample ID	Hand Sample No	$\delta'^{17}O$	$\delta'^{18}O$	$\delta^{17}O$	$\delta^{18}O$	$\Delta'^{17}O$ (λ = 0.528)	$\Delta'^{17}O$ Meas. SE
ID-18-01	1	-0.154	-0.204	-0.154	-0.204	-0.046	0.007
ID-18-02	2	1.523	3.043	1.524	3.048	-0.084	0.007
ID-18-03	3	4.480	8.623	4.490	8.661	-0.074	0.007
ID-18-04a	4						
ID-18-04b	4	4.541	8.781	4.551	8.819	-0.095	0.008
ID-18-05	5	2.997	5.769	3.001	5.786	-0.049	0.008
ID-18-06	6	4.085	7.897	4.094	7.929	-0.085	0.007
ID-18-07a	7	-1.883	-3.532	-1.881	-3.526	-0.018	0.008
ID-18-07b	7						
ID-18-08a	8	-1.897	-3.587	-1.896	-3.580	-0.004	0.008
ID-18-08b	8	4.044	7.803	4.052	7.833	-0.076	0.009
ID-18-09	9	0.529	1.061	0.530	1.061	-0.031	0.006
ID-18-10	10	1.947	3.827	1.949	3.834	-0.073	0.008
ID-18-11	11	2.404	4.655	2.406	4.666	-0.054	0.006
ID-18-12	12	0.556	1.200	0.556	1.201	-0.078	0.008
Quartz Measurements							
Sample ID		$\delta'^{17}O$	$\delta'^{18}O$	$\delta^{17}O$	$\delta^{18}O$	$\Delta'^{17}O$ (λ = 0.528)	$\Delta'^{17}O$ Meas. SE	$\lambda_{quartz\text{-}feldspar}$
ID-18-01		2.778	5.485	2.782	5.500	-0.118	0.009	0.51529
ID-18-02		4.697	9.059	4.709	9.101	-0.086	0.009	0.52764
ID-18-03		4.929	9.480	4.942	9.525	-0.076	0.006	0.52523
ID-18-04a								
ID-18-04b								
ID-18-05		5.430	10.491	5.444	10.547	-0.110	0.008	0.51522
ID-18-06		5.280	10.152	5.294	10.203	-0.080	0.008	0.52986
ID-18-07a		5.509	10.619	5.524	10.675	-0.098	0.008	0.52239
ID-18-07b		5.219	10.008	5.232	10.058	-0.065	0.008	0.52147
ID-18-08a								
ID-18-08b								
ID-18-09		4.024	7.730	4.032	7.760	-0.058	0.007	0.52393
ID-18-10		4.386	8.425	4.396	8.460	-0.062	0.007	0.53053
ID-18-11								
ID-18-12		4.389	8.495	4.399	8.531	-0.097	0.008	0.52543
Standards							
Standard ID	**No.**	**$\delta'^{17}O$**	**$\delta'^{18}O$**	**$\delta^{18}O$**	**$\delta^{18}O$ SD**	**$\Delta'^{17}O$ (λ = 0.528)**	**$\Delta'^{17}O$ SD**
UWG-2	3	3.064	5.910	5.927	0.401	-0.056	0.012
SCO (UNM)	5	2.687	5.189	5.203	0.365	-0.053	0.005
L1 (UNM)	23	9.270	17.735	17.893	0.070	-0.094	0.016
Comparison to Wostbrock et al. (2020) Values							
Standard ID	**$\delta^{18}O$**	**$\delta^{18}O$ SD**	**$\Delta'^{17}O$ (λ = 0.528)**	**$\delta^{18}O$ SD**	**$\delta^{18}O$ Difference**	**$\Delta'^{17}O$ Difference**	
UWG-2	5.696	0.115	-0.071	0.005	-0.231	-0.015	
SCO (UNM)	5.268	0.096	-0.058	0.005	0.065	-0.005	
L1 (UNM)	18.07	0.136	-0.081	0.005	0.177	0.013	

Biotite Measurements		
Sample ID	δD	δD Rep. SE
ID-18-01	-139.9	0.9
ID-18-02	-137.3	4.7
ID-18-03	-106.4	7.3
ID-18-04a	-148.9	3.5

ID-18-04b	-138.2	2.6
ID-18-05	-142.5	1.3
ID-18-06	-129.5	1.1
ID-18-07a	-144.8	2.6
ID-18-07b		
ID-18-08a	-145.7	0.8
ID-18-08b	-145.7	0.8
ID-18-09	-148.5	1.3
ID-18-10	-151.8	1.3
ID-18-11		
ID-18-12	-148.1	3.9

Table S-2 Meteoric Water Line Assumption and Calculated Idaho Batholith Meteoric Waters

Reference	Slope	Intercept	$\delta^{18}O_{mw}$	$\Delta'^{17}O$ (λ = 0.528)	$\delta'^{17}O_{mw}$	$\delta'^{18}O_{mw}$	$\delta^{18}O_{mw}$ SD	$\Delta\delta^{18}O$ [3]	Elevation (km) [4]	SD plus	SD minus	Note
Passey and Ji (2019)	0.528	0.032	-11.920	0.032	-6.320	-11.992	1.106	-5.920	3.11	0.312	-0.377	1, 5
Sharp et al. (2018)	0.52654	0.014	-12.378	0.008	-6.590	-12.455	1.480	-6.378	3.34	0.474	-0.386	2
Luz and Barkan (2010)	0.528	0.037	-12.615	0.037	-6.688	-12.695	1.209	-6.615	3.56	0.544	-0.407	5
Herwartz et al. (2015)	0.5285	0.03	-11.383	0.024	-6.039	-11.448	1.220	-5.383	2.87	0.297	-0.363	
							δD-based Estimate	-10.000	4.74	0.637	-0.487	6

Notes

1 Based on western United States waters that include data in Li *et al.* (2016)

2 Equation as given in text of Sharp *et al*. (2018)

3 Assuming a $\delta^{18}O$ a coastal value of -6 (Mulch *et al*., 2006; Mix *et al*., 2016; Feng *et al*., 2013; Methner *et al*., 2016)

4 Based on propagation through Rowley *et al*. (2001) model

5 By definition, in the λ = 0.528 reference frame, because the slope is 0.528 the $\Delta'^{17}O$ must be equal to the intercept of the MWL.

6 Approximate value for Criss and Taylor (1983) and McFadden *et al.* (2015)

Supplementary Figures

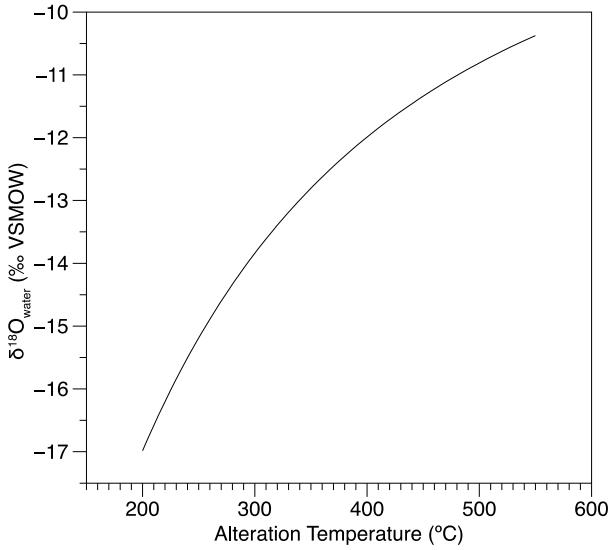

Figure S-1 Sensitivity of calculations to different alteration temperatures via equation S18 using the plagioclase water fractionation factor of Matsuhisa *et al*. (1979) and our derived rock-end-member ($\delta'^{18}O_{rock,final}$ = -9.68, assuming an alteration temperature of 400 °C). Assuming a range of temperatures (*e.g.*, 250 to 500 °C) does not influence the assumed $\delta'^{18}O_{rock,final}$ fitted value (*e.g.,* Figure 3) by more than ~0.3 ‰, though it does require lower (higher) $\delta'^{18}O_{water,final}$ values for lower (higher) temperatures.

Supplementary Information References

Feng, R., Poulsen, C.J., Werner, M., Chamberlain, C.P., Mix, Hari T., Mulch, A. (2013) Evolution of Early Cenozoic topography, climate and stable isotopes of precipitation in the North America Cordillera. *American Journal of Science* 313, 613-648.

Li, S., Levin, N.E., Chesson, L.A. (2015). Continental scale variation in 17O-excess of meteoric waters in the United States. *Geochimica et Cosmochimica Acta* 164, 110-126.

Luz, B., Barkan, E. (2010). Variations of 17O/16O and 18O/16O in meteoric waters. *Geochimica et Cosmochimica Acta* 74, 6276-6286.

Matsuhisa, Y., Goldsmith, J.R., Clayton, R.N. (1979). Oxygen isotopic fractionation in the system quartz-albite-anorthite-water. *Geochimica et Cosmochimica Acta* 43, 1131-1140.

Methner, K., Feibig, J., Umhoefer, P., Chamberlain, P., Mulch, A. (2016) Eo-Oligocene proto-Cascades topography revealed by clumped (Δ47) and oxygen isotope (δ18O) geochemistry (Chumstick Basin, WA, USA). *Tectonics* 35, 546-564. doi:10.1002/2015TCC003984

Mix, H., Ibarra, D., Mulch, A., Graham, S., Chamberlain, C.P. (2016) A hot and high Eocene Sierra Nevada. *Geological Society of America Bulletin* 16, 531-542. doi:10.1130/B31294.1

Passey, B.H., Ji, H. (2019). Triple oxygen isotope signatures of evaporation in lake waters and carbonates: A case study from the western United States. *Earth and Planetary Science Letters* 518, 1-12.

Pack, A. Herwartz, D. (2014) The triple oxygen isotope composition of the Earth mantle and understanding Δ17O variations in terrestrial rocks and minerals. *Earth and Planetary Science Letters* 390, 138–145. doi.org/10/1016/j.epsl.2014.01.017.

Sharp, Z.D. (1990) A laser-based microanalytical method for the in situ determination of oxygen isotope ratios of silicates and oxides. *Geochimica et Cosmochimica Acta* 54, 1353-1357.

Sharp, Z.D., Gibbons, J.A., Maltsev, O., Atudorei, V., Pack, A., Sengupta, S., Shock, E.L., Knauth, L.P. (2016) A calibration of the triple oxygen isotope fractionation in the SiO2-H2O system and applications to natural samples. *Geochimica et Cosmochimica Acta* 186, 105-119.

Sharp, Z.D., Wostbrock, J.A.G. Pack, A. (2018) Mass-dependent triple oxygen isotope variations in terrestrial materials. *Geochemical Perspectives Letters* 7, 27-31.

Taylor, H.P., Jr. (1978) Oxygen and hydrogen isotope systematics of plutonic granitic rocks. *Earth and Planetary Science Letters* 38, 177-210.

Wostbrock, J.A.G., Sharp, Z.D., Sanchez-Young, C., Reich, M., van den Heuvel, D.B., Benning, L.G. (2018) Calibration and application of silica-water triple oxygen isotope thermometry to geothermal systems in Iceland and Chile. *Geochimica et Cosmochimica Acta* 234, 84-97.

Wostbrock, J.A.G., Cano, E.J., Sharp, Z.D. (2020) An internally consistent triple oxygen isotope calibration of standards for silicates, carbonates and air relative to VSMOW2 and SLAP2. *Chemical Geology* 533, 119432.

Yeung, L.Y., Hayles, J.A., Hu, H., Ash, J.L., Sun, T. (2018) Scale distortion from pressure baselines as a source of inaccuracy in triple-isotope measurements. *Rapid Communications in Mass Spectrometry* 32, 1811-1821.

Young, E.D., Galy, A. Nagahara, H. (2002) Kinetic and equilibrium mass-dependent isotope fractionation laws in nature and their geochemical and cosmochemical significance. *Geochimica et Cosmochimica Acta* 66, 1095-1104.